Title

Decellularized Extracellular Matrix Mitigates the Senescent Phenotype and Restores Osteogenic Potential in Human Mesenchymal Stromal Cells

Journal

Journal of Orthopaedic Research, 44(8)

ISSN

0736-0266

Authors

Dorais, CJ

Kruger, NM

Ramos-Rodriguez, DH

et al.

Publication Date

2026-08-01

DOI

10.1002/jor.70264

Decellularized extracellular matrix mitigates the senescent phenotype and restores osteogenic potential in human mesenchymal stromal cells

Connor J. Dorais[1†], Nikolia M. Kruger[1,2†], David H. Ramos-Rodriguez[1], Mark A. Lee[1], and J. Kent Leach[1,2*]

[1]Department of Orthopaedic Surgery, UC Davis Health, Sacramento, CA, USA 95817

[2]Department of Biomedical Engineering, University of California, Davis, Davis, CA, USA 95616

[†]denotes shared first authorship

***Corresponding author**

J. Kent Leach, Ph.D.
UC Davis Health
Department of Orthopaedic Surgery
4860 Y Street, Suite 3800
Sacramento, CA 95817
Email: jkleach@health.ucdavis.edu

ABSTRACT

Autologous cell-based approaches for bone repair using mesenchymal stromal cells (MSCs) in older patients are limited in part by cellular senescence, resulting in impaired MSC self-renewal and differentiation. Currently, the field lacks a standardized method to induce senescence in human MSCs and characterize them for experimental use, as well as effective strategies to mitigate the harmful effects of the senescence-associated secretory phenotype (SASP). We previously demonstrated that MSC-secreted decellularized extracellular matrix (dECM) enhances the osteogenic potential and survival of MSCs. We hypothesized that senescent MSCs would exhibit improved osteogenic potential and reduced SASP activity when maintained on dECM. We first demonstrated that a senescent phenotype can be reliably induced in human MSCs through ionizing irradiation coupled with a 21-day preconditioning phase in culture, evidenced by increased beta-galactosidase staining and enlarged cell area. We then observed that senescent MSCs on dECM exhibit improved osteogenic potential and reduced SASP compared to cells on tissue culture plastic, evidenced by quantifying markers of osteogenic differentiation and ELISAs for known inflammatory cytokines. These data support the promise of dECM as an instructive biomaterial to enhance the regenerative potential of MSCs from older patients for autologous bone repair.

Keywords: senescence, mesenchymal stromal cells, osteogenesis, extracellular matrix, bone

INTRODUCTION

Aging is marked by progressive physiological decline that compromises tissue repair, including the capacity to regenerate bone.[1] Cellular senescence is a key driver of age-associated tissue degeneration, impaired regeneration, and tumorigenesis.[2] Age-related senescence arises from chronic inflammation resulting from the accumulation of stressors such as DNA and mitochondrial damage, triggering stable cell-cycle arrest through telomere shortening and the upregulation of canonical markers, including *p16*, *p21*, and senescence-associated β-galactosidase (SA-β-Gal).[2; 3] Mesenchymal stromal cells (MSCs) are widely studied for use in musculoskeletal repair due to their osteogenic, chondrogenic, and adipogenic potential and secretion of a potent, bioactive secretome.[4; 5] However, MSCs from older donors are scarce and exhibit reduced proliferation and differentiation compared to MSCs from younger donors, largely due to senescence, which impedes their utility for regenerative applications.[6; 7] This altered phenotype limits the use of MSCs from older donors in tissue regeneration approaches.[8]

Cellular senescence is characterized by a state of irreversible proliferative arrest, enlarged cell morphology, granulation, increased SA β-Gal, and the senescence-associated secretory phenotype (SASP).[9; 10] The senescent secretome contains pro-inflammatory cytokines, chemokines, growth factors, proteases, and bio-active lipids.[11] Senescence buildup can be achieved through proliferative exhaustion or external stressors such as reactive oxygen species or irradiation. We previously showed that acute irradiation yields a stress-induced premature senescent (SIPS) MSC phenotype *in vitro* that recapitulates replicative-induced senescence.[12] Although SIPS does not fully capture natural human aging due to mechanistic differences of senescence induction,[13; 14] irradiation is a widely studied stressor for *in vitro* studies because it reliably induces DNA damage and activates senescence response pathways with high reproducibility.[15-17] A hallmark of SIPS is the development of the SASP that is characterized by pro-

inflammatory cytokines such as interleukin-6 (IL-6). Furthermore, we observed that *in vitro* substrate mechanics attenuate IL-6 expression.[16] Other studies indicate that culturing murine MLO-Y4 immortalized osteocytes for 21 days following irradiation-induced senescence is critical for SASP development and manifestation of the senescent phenotype.[15]

The extracellular matrix (ECM) is a cell-secreted network of macromolecules that functions as a reservoir of growth factors and cell adhesion proteins to regulate cellular behavior.[18] We previously demonstrated that cell-derived ECM can be decellularized and harnessed as an instructive biomaterial to promote proliferation and osteogenic differentiation.[19; 20] The decellularized ECM (dECM) is rich in collagen and other matricellular proteins that regulate adhesion, migration, and differentiation. While the transplantation of MSCs from young donors into osteoporotic aged mice reduces MSC senescence and prevents functional bone loss,[21] no studies have reported the use of an instructive biomaterial like dECM to mitigate the senescent phenotype of MSCs and restore their osteogenic potential.

We hypothesized that dECM-mediated cell matrix interactions would mitigate SASP expression and partially restore osteogenic potential of senescent human MSCs. In this study, we first established the role of a preconditioning period to manifest the senescent phenotype in irradiated MSCs. We then examined the capacity of dECM coatings to modulate the function of irradiation-induced senescent MSCs. We tested changes in cell spreading, IL-6 secretion, and osteogenic potential as a function of substrate coating. The results of these studies establish dECM as a promising platform to mitigate the senescent phenotype of human MSCs.

MATERIALS AND METHODS

Cell culture

Human bone marrow-derived mesenchymal stromal cells (Lot #00264, RoosterBio) from a single donor (female, 20 years old) were expanded until passage 5 and used at passage 6-7 in standard culture conditions (37°C, 21% O_2, 5% CO_2) in growth media (GM) composed of alpha minimum essential medium (α-MEM; Life Technologies) supplemented with 10% fetal bovine serum (FBS, Sigma-Aldrich) and 1% penicillin-streptomycin (P/S, 10 mg/mL, Mediatech). Osteogenic media (OM) was composed of GM supplemented with 50 µg/mL L-ascorbic acid-2-phosphate (A2P), 50 µM dexamethasone (DEX), and 500 µg/mL beta-glycerophosphate (BGP).

Production of dECM

MSCs were cultured and expanded for 7 days in GM supplemented with A2P. ECM was generated from MSCs seeded at 50,000 cells/cm^2 in growth media and maintained for 9 days. The ECM was decellularized using a standard detergent removal method described in previous work.[22] Briefly, cells were incubated at 37°C with 0.5% Triton X-100 (Sigma-Aldrich) solution in 20 mM ammonium hydroxide (NH_4OH) (Fluka 09859) in phosphate buffered saline (PBS), followed by treatment with 0.1 mg/mL DNase I (MilliporeSigma) in PBS supplemented with 0.1 g/L $CaCl_2$ at 37°C and three PBS washes. Following 1 h incubation in DNase, ECM was extracted with a cell scraper and collected in 0.02 N acetic acid, sonicated until mixture was homogeneous, and stored at -20°C until use.[23]

Induction of senescence

MSCs were lifted with trypsin, resuspended in GM at 1x10^6 cells/mL, and subjected to 10 Gy irradiation once. Irradiated MSCs were referred to as irradiated stress-induced senescent MSCs (IRR MSCs). IRR MSCs were cultured for 21 d at a density of 6.82x10^5 cells/mL in T300 flasks to establish the senescent phenotype (preconditioning phase) and then lifted and reseeded in 24-well plates at 5x10^5 cells/cm^2. For immunofluorescence staining, IRR MSCs were reseeded

in 96-well glass-bottom plates at 80 cells/mm^2. Wells were coated with rat tail collagen 1 (MilliporeSigma, St. Louis, MO) or dECM at 30 µg/cm^2. Cultures were maintained in standard culture conditions, and media was refreshed every 2-3 d.

MSC viability and metabolism

DNA content was quantified after lysing MSCs with 1X passive lysis buffer (PLB) (Promega, Minneapolis, MN), followed by sonication for 10 s and centrifugation at 5,000x*g* at 4°C for 5 min to obtain a cell debris pellet. DNA was extracted from the supernatant and Quant-iT dsDNA kit (Invitrogen, Waltham, MA). Metabolic activity was measured using alamarBlue (Invitrogen) following manufacturer's instructions.

Senescence associated β-Galactosidase staining

Preconditioned IRR MSCs were seeded in 24-well plates at 2x10^5 cells/well and maintained for 1, 7, 14 and 21 d. At each time point, cells were washed with PBS and fixed with 10% buffered formalin phosphate for 30 min. Samples were then stained using the Senescence Associated β-Galactosidase Staining Kit (Cell Signaling Technology, Danvers, MA) according to the manufacturer's instructions and imaged (Nikon Eclipse, TE2000U).

Quantitative polymerase chain reaction (qPCR)

Samples were collected in 300 µL of TRIzol (Invitrogen) and homogenized by sonication (Sonics, Newton, CT) for two 10 s intervals. RNA was isolated following manufacturer instructions. 800 ng of mRNA was reverse transcribed utilizing the QuantiTect Reverse Transcription Kit

(Qiagen, Hilden, Germany) and diluted to a final concentration of 12 ng/µL. qPCR was performed using Taq PCR Master Mix (Qiagen) in a QuantStudio 6 Pro real-time PCR system (ThermoFisher). Single primers were purchased from ThermoFisher Scientific, and we quantified expression of interleukin-6 (*IL-6,* Hs0107564_m1*),* cyclin-dependent kinase inhibitor 1A *(CDKN1A* (p21)*,* Hs00355782_m1*),* cyclin-dependent kinase inhibitor 2A *(CDKN2A* (p16)*,* Hs00923894_m1), collagen type 1 (*COL1A1*, Hs00164004_m1) and osteopontin (*SPP1*, Hs00959010_m1). Critical threshold values (Ct) were quantified for each gene of interest, and the ΔCt for each sample was calculated by subtracting the sample's Ct value of the housekeeping gene, *GAPDH*. The ΔΔCt value of each sample was quantified by subtracting the average ΔCt value of the day 1 IRR MSC group on TCP. Expression of each gene was calculated and presented as $2^{-\Delta\Delta Ct}$. The same process was used to analyze integrin gene expression. Primers were purchased from ThermoFisher Scientific and expressions of integrin beta 3 (*ITGB3*, Hs01001469_m1), integrin beta 1 *(ITGB1,* Hs01127536_m1), integrin alpha 2 (*ITGA2*, Hs00158127_m1), integrin alpha 5 (*ITGA5*, Hs_01547673_m1), integrin alpha V (*ITGAV,* Hs00233790_m1) were measured. The ΔΔCt value of each sample was quantified by subtracting the average ΔCt value from the D0 healthy MSC group. Expression of each gene was calculated and presented as $2^{-\Delta\Delta Ct}$.

Quantification of IL-6 secretion from MSCs

Cultures were maintained in 24-well plates with 1 mL OM media. Wells were refreshed with half the volume of media (0.5 mL) 24 h prior to collection, and conditioned media was collected on days 1, 7, 14, and 21. Secretion of IL-6 was quantified using a human specific IL-6 enzyme-linked

immunosorbent assay (ELISA) kit (R&D Systems, Minneapolis, MN) per the manufacturer's instructions and quantified in a Synergy HTX multi modal plate reader.

Osteogenic differentiation and mineralization assays

Intracellular alkaline phosphatase (ALP) activity was quantified and normalized to total DNA content measured using the Quant-iT PicoGreen dsDNA Assay Kit (Invitrogen). For Alizarin Red S staining, wells were fixed in 10% formalin for 30 min at room temperature then rinsed with distilled water. Alizarin Red staining solution was prepared by dissolving 2 g Alizarin Red (Sigma, A5522) in 100 mL distilled water, adjusting the pH to 4.1 using 400 µL of 0.5 N ammonium hydroxide (Sigma, 221228). Wells were incubated with 2% Alizarin Red solution for 30 min, washed twice with distilled water, then imaged at 10x magnification using a brightfield microscope. Destaining solution (110 µL of 10% cetylpyridinium chloride in 10 mM sodium phosphate, pH 7.0) was added to each well for 15 min at room temperature. Eluted solution was mixed and transferred to 96-well plate for quantification at 405 nm. For quantitative calcium deposition quantification, samples were digested in 1 M HCl for 48 h, and calcium content was measured using a StanBio Calcium Liquid Reagent kit (Thermo Fisher, Chicago, IL).

Immunofluorescence staining, and confocal imaging

Healthy MSCs were expanded for 5-7 d to reach confluence prior to lifting and seeding on 96-well glass bottom plates. Stress-induced senescent MSCs were generated following irradiation and a 21-day preconditioning phase prior to lifting and seeding on 96-well glass bottom plates. Following seeding, cells were cultured for 24 h before fixation overnight at 4°C with 4% paraformaldehyde (PFA). PFA was then removed and replaced with PBS. MSCs were permeabilized with 0.1% Triton X-100 in 2 mM $CaCl_2$ for 10 min at room temperature then rinsed twice with PBS before the samples were blocked with a 10% goat serum/1% bovine serum

albumin (BSA) solution for 30 min at room temperature. Samples were subsequently incubated overnight at 4ºC with vinculin monoclonal antibody (Invitrogen, 14-9777-80, 1:150) and phosphorylated focal adhesion kinase (Phospho-FAK Tyr397) monoclonal antibody (Invitrogen, 700255, 1:400). Samples were then stained with goat anti-rabbit secondary antibody (Alexa Fluor Plus 647; Invitrogen, A32733, 1:400) and goat anti-mouse secondary antibody, Alexa Fluor 555 (Invitrogen, A21422, 1:400) for 1 h at room temperature (RT). Samples were then stained with Alexa Fluor 488 phalloidin (Invitrogen, A12379, 1:500) for 1 h at RT and then DAPI (Invitrogen, D1306, 1:2500) for 10 min at RT. All stained samples were washed with PBS and imaged on a Stellaris 5 confocal microscope with a 40x water immersion objective (Leica Stellaris 5, Wetzlar, Germany). Laser and imaging settings were kept consistent across groups. Images were acquired as z-stacks at 0.2 µm intervals.

Cell area quantification

Following confocal imaging of MSCs seeded on TCP for 24 h, F-actin micrographs were processed in ImageJ to quantify single-cell area. Using automated thresholding, we segmented the cell body for healthy and IRR single cells on TCP. Threshold images were converted to binary masks and “Fill Holes” algorithm was applied to generate continuous cell objects. Edges were then delineated using the “Find Edges” function. Cell area (μm^2) was quantified using the “Analyze Particles” function on all processed images.

Statistical analysis

Data are presented as the means ± standard deviation. Statistical analysis was performed using GraphPad Prism 10.2.3 software (GraphPad Software, Boston, MA) to conduct one-way or two-way analysis of variance (ANOVA) for multiple comparisons or Student’s t-test when

appropriate. Comparisons made within groups and conditions were analyzed through Pearson's correlation coefficient (two-way ANOVA) or Tukey's post-hoc test (one-way ANOVA). Experiments to assess integrin gene expression were performed once with three technical replicates from a single biological replicate. Given the limited number of technical replicates (n=3) and non-normal distribution of data, the Kruskal-Wallis test was used to compare medians between groups. The adjusted p-value and corresponding first and third quartile values are reported. p-values <0.05 were considered statistically significant. Different letters denote statistical significance between groups, while data sharing a letter are not statistically different from one another.

RESULTS

Preconditioning of irradiated cells manifests the senescent phenotype in human MSCs

We generated senescent cells by subjecting passage 6 healthy human MSCs once to 10 Gy ionizing irradiation (**Figure 1A-i**). Irradiated MSCs underwent a 21-day preconditioning phase in growth media to develop and stabilize the senescent phenotype (**Figure 1A-ii**). Senescent and healthy cells were seeded on uncoated TCP well plates or TCP coated with COL or dECM to evaluate how substrate composition influences adhesion, morphology, SASP production, and recovery of osteogenic potential (**Figure 1A-iii**). Over the 21-day preconditioning period, we observed significant morphological changes in irradiated MSCs (IRR) compared to their healthy counterparts (**Figure 1B**). Morphological differences between healthy and irradiated cells were indistinguishable after 1 day. However, over 21 days, IRR MSCs were less confluent, and exhibited more granulation compared to healthy cells that possessed high confluency. After reseeding onto TCP, IRR MSCs were significantly larger in cell area (IRR TCP, 17,279 ± 8014 μm^2; Healthy TCP, 3076 ± 1515 μm^2, p=0.013) (**Figure 1C**), while healthy cells exhibited an elongated shape. Neither *p21* (*CDKN1A*) nor *p16* (*CDKN2A*) expression in IRR MSCs showed a continuous increase over

the 21-day culture period. *CDKN1A* gene expression was elevated at early timepoints (days 1 and 7) but trended toward healthy MSC levels by days 14 and 21. *CDKN2A* expression did not show sustained elevation relative to healthy MSCs over the culture duration (**Figure S1**). Over this same preconditioning duration, we observed increased SA-β-Gal staining in IRR MSCs (**Figure 1D**), collectively validating the stabilization of the senescent phenotype.

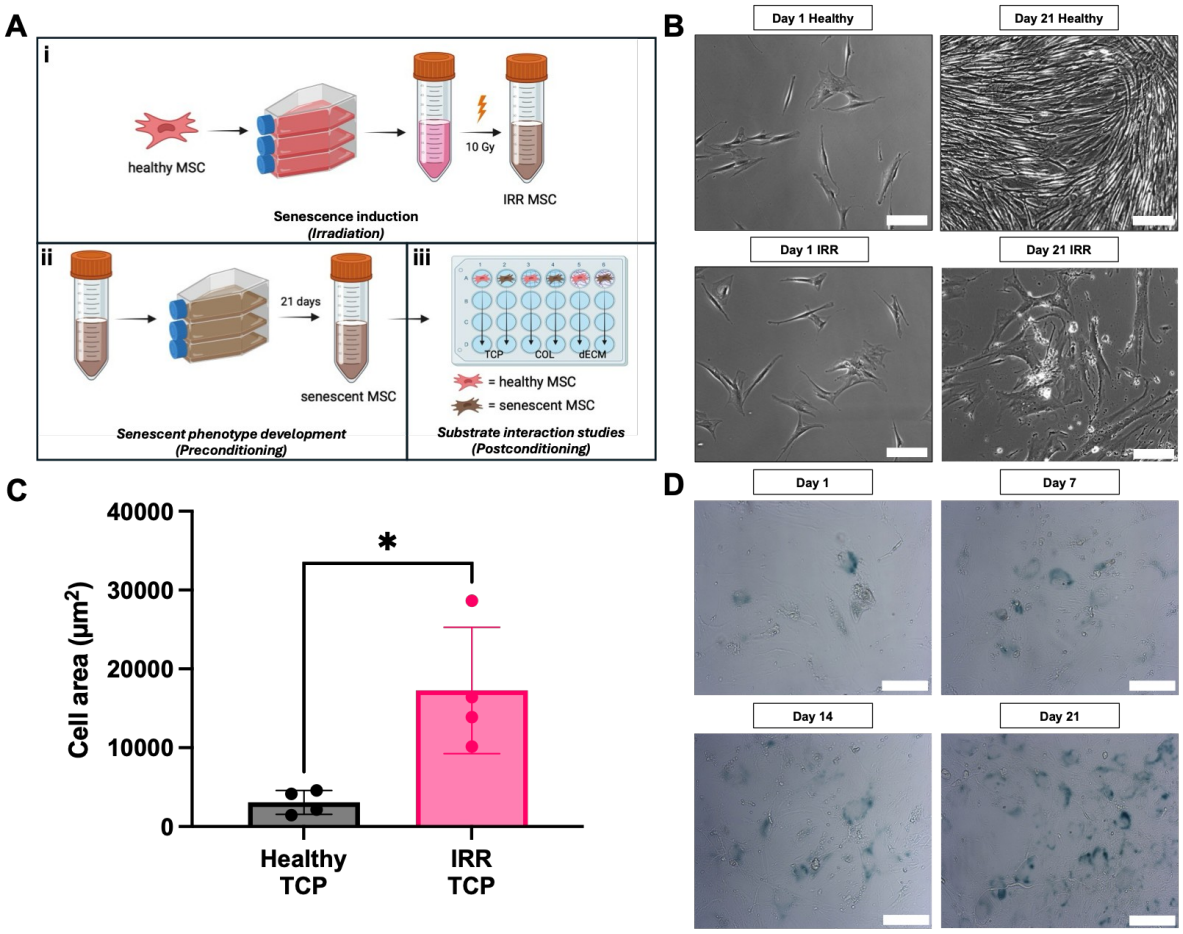

Figure 1. Induction of senescence through irradiation and 21-day preconditioning culture period. (**A**) (**i**) Schematic diagram of senescence induction in MSCs by irradiation**;** (**ii**) Preconditioning for 21 days to allow development of SASP**;** (**iii**) 21-day culture period to assess MSC interaction with distinct substrates. (**B**) Brightfield images of healthy and IRR MSCs before and after 21 days of preconditioning. Top row is healthy MSCs; bottom row is irradiated MSCs.

Scale bar represents 200 μm. (**C**) Quantification of healthy and IRR MSC cell area on TCP at 24 h post seeding. (**D**) Senescence Associated β-Galactosidase staining of IRR MSCs throughout the preconditioning phase. Scale bar represents 250 μm. Statistics: unpaired t test. *$p < 0.05$. Data are presented as mean ± standard deviation (n=4). **TCP**, tissue culture plastic; **IRR**, irradiated MSCs.

Integrin expression and MSC adhesion is altered by senescence and substrate composition

Healthy and senescent MSCs were cultured for 24 hours on TCP, COL, or dECM to assess changes in actin fiber organization, vinculin distribution, and phosphorylated focal adhesion kinase (pFAK) localization. Healthy MSCs, regardless of substrate, exhibited similar vinculin staining patterns (**Figure 2A**), yet pFAK activation was greatest for healthy MSCs on dECM. Focal adhesions remained evenly distributed, coinciding with organized actin stress fibers. While COL supported moderate pFAK activation, dECM further enhanced pFAK signaling, demonstrating substrate-dependent adhesion signaling without corresponding changes in vinculin localization. Senescent MSCs exhibited clearer substrate-dependent differences in focal adhesion localization and pFAK activation (**Figure 2A**). Cells cultured on dECM showed the most robust and well-defined vinculin and pFAK localization, indicating enhanced adhesion signaling on biologically relevant matrices. Senescent cells on COL and TCP exhibited reduced vinculin expression and pFAK localization compared to MSCs on dECM. These observations suggest that senescent MSCs on dECM form localized and active adhesion sites with heightened pFAK activation, whereas cells on more homogeneous substrates form larger, adhesions with reduced kinase activity. Comparatively, healthy MSCs on dECM exhibited more pronounced pFAK activation, but formed less localized adhesion sites across all substrate types.

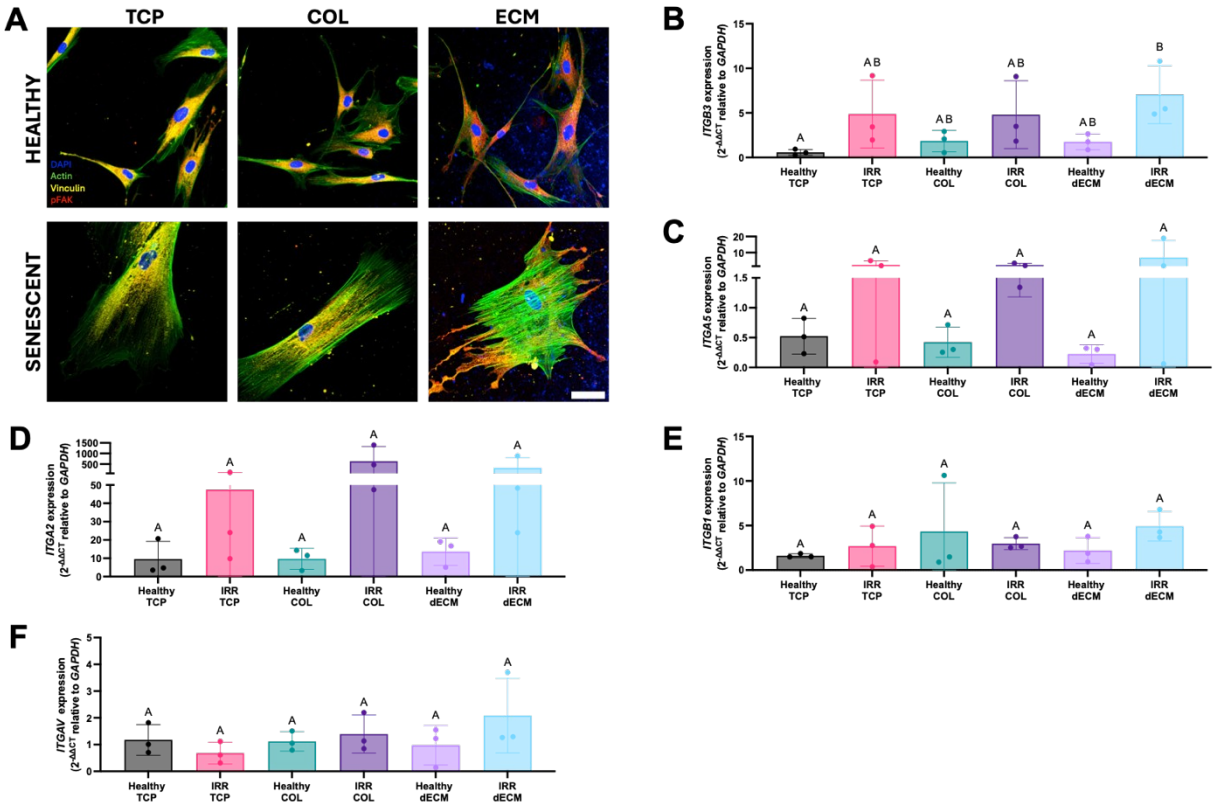

Figure 2. Integrin expression is modulated by senescence, while substrate composition modulates focal adhesion signaling. (**A**) Maximum projection images of healthy and senescent MSCs on TCP, COL, and dECM; DAPI (blue), phalloidin (green), vinculin (yellow), pFAK (red). Scale bar represents 50 µm. Gene expression of integrin subunits (**B**) *ITGB3,* (**C**) *ITGA5,* (**D**) *ITGA2* (**E**) *ITGB1* (**F**) *ITGAV* for MSCs on TCP, COL or dECM. Statistics: bars with different letters are statistically different from each other. Data are presented as mean ± standard deviation (n=3). **TCP**, tissue culture plastic; **COL**, collagen; **dECM**, decellularized ECM; **IRR**, irradiated MSCs.

To evaluate how substrate composition influences integrin expression, we measured gene expression of key integrin subunits beta 3, alpha 2, alpha 5, alpha V, and beta 1 in healthy and senescent MSCs. Regardless of substrate, *ITGB3, ITGA5*, and *ITGA2* expression tended to be higher in senescent cells than in healthy cells, yet only *ITGB3* expression in senescent cells on

dECM was elevated relative to healthy cells on TCP (p=0.043). Median (Q1–Q3) values were 0.536 (0.284–0.933) for healthy cells on TCP and 5.47 (4.879–10.806) for senescent cells on dECM. Similar trends were observed with *ITGA5* expression, where healthy cells showed no upregulation for any substrate, yet senescent MSCs, regardless of substrate showed slight upregulation, with dECM inducing the greatest change. *ITGA2* expression in senescent MSCs exhibited modest upregulation in senescent cells on COL and dECM relative to healthy cells, though these differences were less pronounced between healthy and senescent cells on TCP (**Figure 2B-D**). *ITGB1* expression was upregulated for both cell types relative to D0 healthy cells prior to seeding on any substrate. However, the relative upregulation was similar between healthy and senescent cells, regardless of substrate (**Figure 2E-F**). Similar trends were observed for *ITGAV* expression, although there was less upregulation compared to D0 healthy cells. These data reveal that senescent cells on dECM preferentially upregulate *ITGB3* to bind to the matrix.

dECM mitigates the senescent phenotype of irradiated human MSCs

The senescent phenotype is commonly characterized by beta-galactosidase production, expression of p16 and p21, and secretion of a pro-inflammatory SASP.[24] As the SASP is the functional manifestation of senescence, we sought to determine if the SASP of IRR MSCs can be reduced through cell-substrate interactions. We first evaluated gene expression of *CDKN1A* and *CDKN2A,* which encode for p21 and p16, respectively. *CDKN1A* expression was unchanged in IRR MSCs across all substrates after 21 days (**Figure 3A**). *CDKN2A* expression was reduced when IRR MSCs were cultured on dECM compared to COL, yet expression was similar for cells on dECM and TCP (**Figure 3B**).

Human IL-6 gene and protein expression levels were also assessed for IRR MSCs cultured on TCP, COL and dECM to determine if primary components of the SASP could be lessened by interaction with dECM (**Figure 3C**). IL-6 gene expression in IRR MSCs was reduced after 21 days in culture on dECM compared to COL but not compared to TCP. IL-6 protein levels were reduced on all substrates over time (**Figure 3D-F**). However, IL-6 expression was reduced in IRR MSCs cultured on TCP and dECM compared to COL, suggesting dECM can mitigate the senescent phenotype (**Figure 3F**).

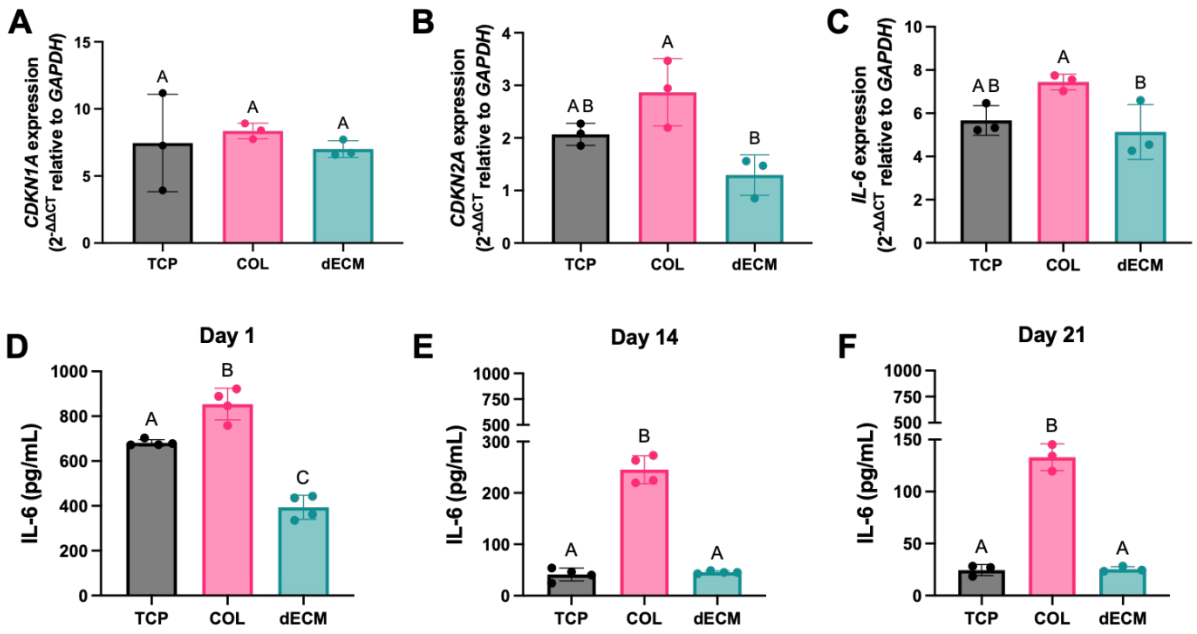

Figure 3. Culture of irradiated MSCs on dECM mitigates expression of SASP markers. Expression of senescent genes (**A**) *CDKN1A*, (**B**) *CDKN2A*, and (**C**) *IL-6* after 21 days on dECM. (**D, E, F**) Human IL-6 gene expression and protein secretion throughout 21-day postconditioning culture period. Statistics: bars with different letters are statistically different from each other. Data are presented as mean ± standard deviation (n=3-4). **TCP**, tissue culture plastic; **COL**, collagen; **dECM**, decellularized ECM; **IRR**, irradiated MSCs.

dECM can restore the osteogenic potential of senescent MSCs

We characterized expression of common osteogenic genes (*COL1A1* and *SPP1*) in irradiated MSCs after 21 days in osteogenic media on various substrates. Although *COL1A1* expression was not different among sample groups at the same time point, we observed an upregulation of *COL1A1* from day 1 to day 21 (**Figure 4A**). At the gene level, *SPP1* exhibited the highest expression in IRR MSCs on dECM at day 21 ($p<0.0001$). *SPP1* expression was significantly higher on day 21 compared to day 1 ($p<0.0001$) and higher when IRR MSCs were cultured on dECM compared to COL (**Figure 4B**). Osteogenic differentiation was also analyzed through quantification of intracellular ALP activity, which revealed an upregulation for IRR MSCs on dECM (TCP: 0.006 ± 0.0002; COL: 0.001 ± 0.0007; dECM: 0.015 ± 0.002 U/ng DNA; $p<0.01$). After 14 days in osteogenic media, IRR MSCs on dECM expressed more ALP than on COL by 1.6-fold and TCP by 2.5-fold (**Figure 4C**). We detected a trend for increased calcium deposition after 21 days for IRR MSCs on dECM compared to COL (TCP: 2.1 ± 0.2; COL: 1.8 ± 0.1; dECM: 2.6 ± 0.4 µg) (**Figure 4D**). We observed mineralization of IRR MSCs qualitatively by Alizarin Red S staining and quantitatively upon solubilization of the stain. In agreement with ALP activity and calcium deposition, stain quantification revealed higher mineral deposition of IRR MSCs on dECM than on COL and TCP (TCP: 0.008 ± 0.0002; COL: 0.001 ± 0.003; dECM: 0.012 ± 0.001 RFU/ng DNA; $p<0.01$) (**Figure 4E**). Darker hues of red staining further confirmed the osteogenic differentiation of IRR MSCs when cultured on dECM compared to COL and TCP (**Figure 4F**). Independent of substrate, IRR MSCs exhibited reduced calcium deposition as well as lower Alizarin Red S staining and quantification relative to healthy MSCs on TCP, indicating impaired osteogenesis for senescent cells (**Figure 4D-F**).

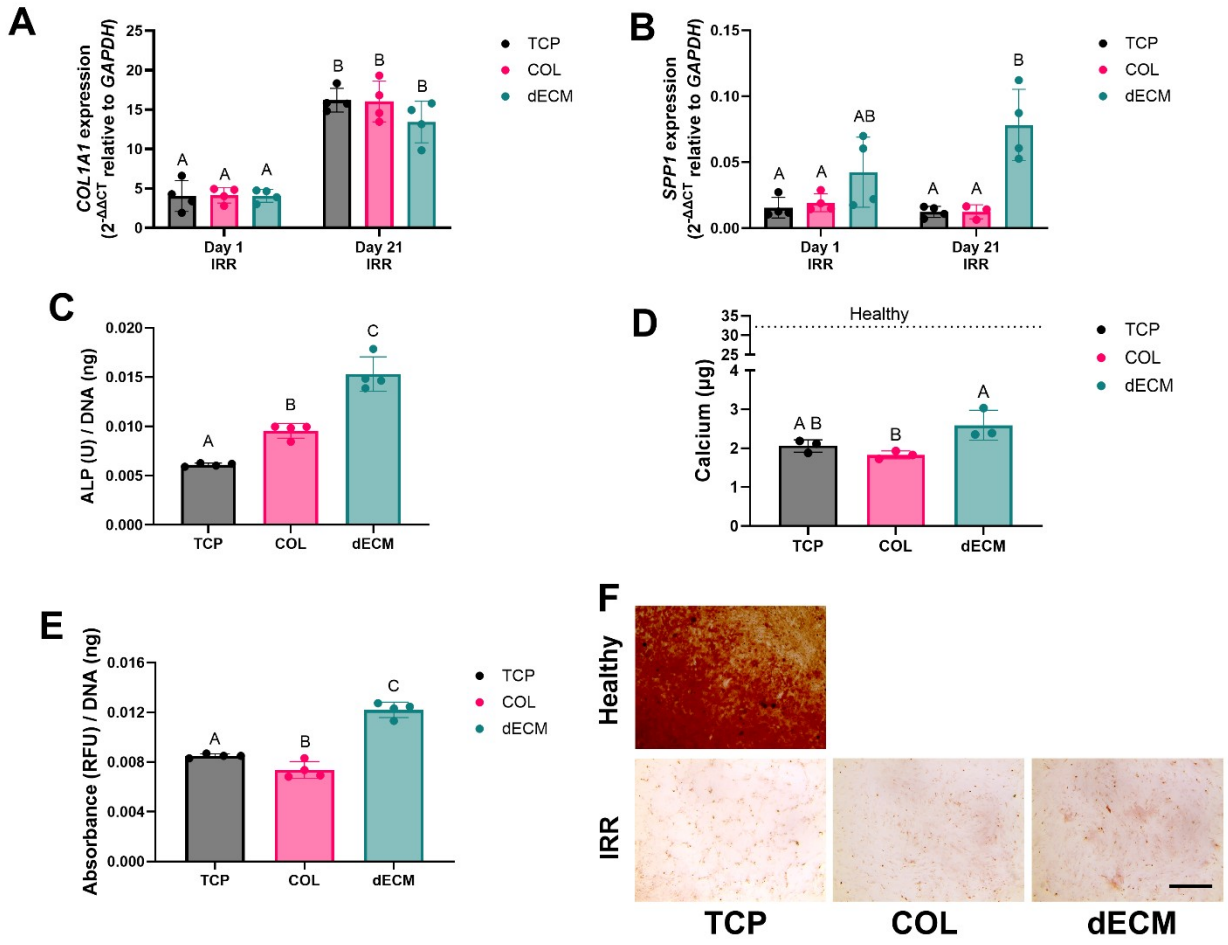

Figure 4. dECM improves osteogenic potential of senescent IRR MSCs. Expression of osteogenic genes (**A**) *COL1A1* and (**B**) *SPP1* in IRR MSCs after 21 days in osteogenic media. (**C**) ALP activity, (**D**) calcium deposition and **(E)** Alizarin Red S quantification and (**F**) staining were also used to characterize changes in osteogenic potential. Statistics: bars with different letters are statistically different from each other. Data are presented as mean ± standard deviation (n=3-4). **TCP**, tissue culture plastic; **COL**, collagen; **dECM**, decellularized ECM; **IRR**, irradiated MSCs.

DISCUSSION

Mesenchymal stromal cells (MSCs) are widely used in cell therapy due to their accessibility and pro-regenerative functions, yet the effects of cellular senescence on their therapeutic performance remain poorly understood. Cellular senescence is characterized by durable cell cycle arrest and phenotypic remodeling including metabolic dysregulations, impaired lineage commitment, and acquisition of a SASP.[8] For musculoskeletal regeneration, the SASP is known to diminish osteogenic capacity, disrupt mechanosensing, and induce paracrine activity that promotes chronic inflammation and ECM degradation.[25] The role of ECM as primary driver of MSC fate through integrin engagement, growth-factor sequestration and presentation, and biophysical signaling[18; 23; 26; 27] makes dECM a compelling strategy to instruct senescent cells toward a more pro-regenerative state. By providing a native-like composition and architecture, dECM can modulate adhesion-dependent signaling, dampen inflammatory cues, and restore aspects of osteogenic differentiation that are diminished with senescence.

Cellular senescence in human MSCs has been induced using numerous techniques including culturing cells to high passage (replicative senescence), hydrogen peroxide, etoposide, and irradiation-induced senescence.[12;28] For this study, irradiation was employed as a reproducible model of stress-induced premature senescence.[29] We and others reported that irradiation is a reliable method to induce pre-senescent MSCs, activating early senescence-associated pathways.[12; 16; 30] Herein, we show that a 21-day preconditioning period is necessary following irradiation to develop and stabilize the senescent phenotype in human MSCs. To confirm the senescent phenotype, proper validation is required by analysis of known pro-inflammatory markers and common approaches such as SA-β-Gal staining and cell morphology analysis.[31] After irradiation and a 21-day preconditioning phase, we noted hallmark characteristics of senescence such as halted proliferation, enlarged cell area, and granulation. Furthermore, we observed increased SA-β-Gal staining in the irradiated MSC population over the 21-day

preconditioning period. During the study, it became evident that careful consideration of cell seeding density is required to elucidate reliable staining results, as both high and low cell confluence can cause false-positive or false-negative results, respectively.[31] This 21-day preconditioning phase is necessary to develop and stabilize the senescent phenotype, as there are no absolute mechanisms to achieve this state beyond replicative senescence. These data are in agreement with prior work in which nearly 100% of irradiated murine MLO-Y4 osteocytes demonstrated positive SA-β-Gal staining after 20 days.[15] The improved consistency in senescent characteristics within immortalized osteocytes compared to human MSCs may be due to heterogeneity of the MSC culture compared to the homogeneous cell line. The lack of definitive markers for senescence in human MSCs highlights the field's need for reproducible and efficient experimental techniques for senescence induction, as provided by this 21-day preconditioning regimen.

We previously reported that dECM is an effective biomaterial to enhance proliferation, viability, metabolic activity, and osteogenesis in healthy human MSCs through instructional cues.[19; 26] dECM mimics the native complex microenvironment that fosters mechanical and biochemical cues that supports cell adhesion, growth, and differentiation.[18; 32] Since dECM can mimic the native, healthy environment that is often degraded or dysfunctional in aged or diseased tissues, this motivated our study of its potential to alleviate the detrimental senescent phenotype and restore osteogenic capabilities to senescent-induced MSCs.

To better understand how senescent cells engage their surrounding substrates, we assessed adhesion and signaling responses of senescent cells on TCP, COL and dECM relative to healthy cells using immunofluorescence and qPCR. Previous work by Gresham *et al.* demonstrated that vinculin expression and F-actin fiber alignment differ between irradiated and healthy MSCs,[16] likely due to cytoskeletal remodeling and altered focal adhesion organization in

senescent MSCs.[33; 34] Consistent with these observations, senescent cells exhibited substrate-dependent differences in vinculin localization and pFAK activation. Senescent cells cultured on dECM possessed strong, well-defined vinculin plaques and pFAK localization at the periphery of the cell, suggesting the formation of more well-defined focal adhesions in contrast to cells on TCP and COL with diffuse vinculin levels and limited pFAK signal. These findings indicate that substrate composition can influence focal adhesion organization and associated signaling, particularly in senescent MSCs. In contrast, healthy MSCs had less pronounced substrate-dependent differences in adhesion structure, despite slight detectable differences in kinase activity. Together, these findings suggest that senescent MSCs may be more sensitive to substrate composition as it relates to focal adhesion organization while both healthy and senescent cells show substrate-dependent signaling differences.

To further understand how senescent cells interact with their surroundings, we measured expression of integrin-encoding genes 24 h post-seeding to assess early transcriptional changes between healthy and senescent cells across substrates. Both healthy and senescent cells upregulated *ITGB1* and *ITGAV*, consistent with their role as broad adhesion receptors. In contrast, senescent cells preferentially upregulated *ITGB3, ITGA2* and *ITGA5* relative to healthy MSCs, suggesting an early shift in adhesion dynamics for senescent cells. The increase in *ITGB3* expression is consistent with prior reports identifying the β3 integrin subunit as a regulator of senescence and is upregulated in senescent human primary fibroblast cells.[35] However, trends for expression of *ITGB1*, *ITGAV*, *ITGA2*, and *ITGA5* in senescent human MSCs remain poorly characterized, as many studies explore the role of ECM composition or aging in cell adhesion rather than directly comparing integrin transcriptional changes between senescent and healthy cells cultured on specific substrates.[36; 37] The observed variability in gene expression within the senescent cell population likely reflects known heterogeneity within the senescent cell

population.[38] Future work should focus on single-cell RNA sequencing to study integrin gene expression in senescent cells exhibiting the same senescent markers. Moreover, because this study was limited to transcriptional assessment, future studies to correlate gene and protein level abundance or localization will be necessary to further understand the relationship of integrins with senescent cell behavior.

Consistent with previous findings, we noted the detrimental effects of the SASP through the secretion of proteins involved in inflammation such as IL-6.[39] Prior work demonstrated the capability of softer substrates to mitigate the secretion of this pro-inflammatory cytokine.[16] Leveraging this knowledge, we sought to understand how dECM could be used as an instructive, biologically relevant cue to mitigate the SASP. In our 21-day postconditioning culture phase, we noted an initial upregulation of *IL-6* gene expression in irradiated MSCs, confirming the development of the senescent phenotype. However, over the course of 21 days, we detected a drastic reduction in *IL-6* expression when irradiated MSCs were cultured on dECM, suggesting that dECM could mitigate one of the primary pro-inflammatory cytokines indicative of the SASP. We also assessed the influence of dECM on common senescence genetic markers (i.e., *CDKN1A*, *CDKN2A*, *IL-6*). Although we did not detect transcriptional changes for *CDKN1A*, we observed a decrease in both *CDKN2A* and *IL-6* expression in irradiated MSCs on dECM compared to TCP. This further validates the use of dECM in mitigating senescence and SASP components. Senescence is heterogeneous, and many commonly used markers are context-dependent and inconsistent across conditions.[40] These limitations underscore the need for an accessible, robust biomarker and for defining the specific dECM components that modulate senescence to improve reproducibility and mechanistic insight.

The SASP has detrimental effects that hinder cell differentiation. Therefore, we explored how dECM can be used to restore osteogenic potential as it did for senescence and SASP

recovery. While *COL1A1* increased over time, we did not detect differences in expression in cells as a function of substrate. However, we did measure significant increases in *SPP1* for IRR MSCs on dECM over 21 days compared to cells on tissue culture plastic or collagen. When analyzing ALP activity and mineralization, we observed significant increases when senescent MSCs were cultured on dECM. These results suggest that dECM can partially restore the osteogenic potential of irradiation-induced senescent human MSCs.

Although these findings support the use of dECM as an instructive biomaterial to recover the SASP and osteogenic potential of senescent cells, there are limitations to the study that merit further investigation. Notably, the use of MSCs from a single young donor limits direct comparison to age-associated senescence. While MSCs from aged donors more closely reflect chronological aging, they are often associated with reduced differentiation potential, increased baseline senescence, and substantial heterogeneity, which can complicate controlled mechanistic studies. Therefore, this study utilized MSCs from young donors for consistency.[41-43] Future studies incorporating aged donor MSCs will be necessary to determine differences between chronological aging and acute irradiation-induced senescence. Reliable and consistent markers for determining senescence remain elusive. The senescent phenotype is variable and heterogeneous on a single-cell level, making it difficult to accurately characterize and target with a limited set of available biomarkers.[44] Furthermore, commonly studied senescent markers like *CDKN1A* and *CDKN2A* are reliable markers in some models but are less consistent in human MSCs.[29] Gene expression of *CDKN2A* and *CDKN1A* in human MSCs exhibit variability due to donor heterogeneity and context-dependent activation of senescence-associated pathways, thereby contributing to observed fluctuations in gene expression.[38; 45] Currently, the most comprehensive strategy is to assess and quantify multiple senescence hallmarks within the same samples, as in this study. However, this multi-parameter approach is experimentally demanding and difficult to standardize. Identifying a

universal, targetable marker of senescence is therefore critical to streamline experimental design and accelerate development of therapies to attenuate senescence when using human MSCs. The use of dECM as a biomaterial demonstrates high potential to attenuate the detrimental effects of the SASP, yet dECM is presently difficult to produce in large, homogeneous batches. Current strategies for bulk production of dECM are limited by batch-to-batch culture processes, variable composition, and inconsistencies in bioactivity.[46] Future studies must investigate specific pro-inflammatory markers of the SASP and components of dECM to provide consistency.

CONCLUSION

We demonstrated the reproducibility of stabilizing the senescent phenotype through irradiation and a 21-day preconditioning phase. We further showed that senescent MSCs cultured on dECM exhibited localized focal adhesions and increased kinase activation, providing a mechanistic insight into how these cells engage their surroundings. Through this enhanced cell-dECM interaction, we modulated the behavior of irradiation-induced senescent MSCs by both reducing the SASP pro-inflammatory environment and increasing their osteogenic potential. This highlights the importance of the dECM as a biomaterial to mitigate the inflammatory secretome and improve the osteogenic potential of irradiation-induced senescent MSCs. Understanding how senescent MSCs respond to dECM is critical for advancing dECM-based therapies for bone regeneration, particularly when working with senescent cells or older donor cell populations.

Acknowledgements

JKL acknowledges financial support from the Lawrence J. Ellison Endowed Chair of Musculoskeletal Research.

Author contributions

Connor Dorais: Methodology, Investigation, Validation, Data curation, Formal analysis, Writing- Original draft preparation. **Nikolia Kruger:** Methodology**,** Investigation, Validation, Data curation, Writing- Original draft preparation. **David Ramos-Rodriguez:** Methodology, Investigation, Validation, Formal analysis Writing- Reviewing and Editing. **Kent Leach:** Conceptualization, Resources, Supervision, Writing- Reviewing and Editing.

Competing interests

The authors declare they do not have any competing interests.

Data and materials availability

The dataset generated and/or analyzed during the current study are available from the corresponding authors upon reasonable request.

Supporting information

Additional supporting information can be found online in the Supporting Information section.

References

1. Pignolo RJ, Law SF, Chandra A. 2021. Bone aging, cellular senescence, and osteoporosis. JBMR Plus 5:e10488.

2. Campisi J. 2013. Aging, cellular senescence, and cancer. Annu Rev Physiol 75:685–705.

3. Campisi J, Robert L. 2014. Cell senescence, role in aging and age-related diseases. Interdiscip Top Gerontol 39:45.

4. Pittenger MF, Mackay AM, Beck SC, et al. 1999. Multilineage potential of adult human mesenchymal stem cells. Science 284:143–147.

5. Caplan AI, Dennis JE. 2006. Mesenchymal stem cells as trophic mediators. J Cell Biochem 98:1076–1084.

6. Kim M, Kim C, Choi YS, et al. 2012. Age-related alterations in mesenchymal stem cells related to shift in differentiation from osteogenic to adipogenic potential: implication to age-associated bone diseases and defects. Mech Ageing Dev 133:215–225.

7. Stenderup K, Justesen J, Clausen C, et al. 2003. Aging is associated with decreased maximal life span and accelerated senescence of bone marrow stromal cells. Bone 33:919–926.

8. Weng Z, Wang Y, Ouchi T, et al. 2022. Mesenchymal stem/stromal cell senescence: hallmarks, mechanisms, and combating strategies. Stem Cells Transl Med 11:356–371.

9. Coppé J-P, Desprez P-Y, Krtolica A, et al. 2010. The senescence-associated secretory phenotype: the dark side of tumor suppression. Annu Rev Pathol 5:99–118.

10. Gnani D, Crippa S, Della Volpe L, et al. 2019. An early-senescence state in aged mesenchymal stromal cells contributes to hematopoietic stem and progenitor cell clonogenic impairment through the activation of a pro-inflammatory program. Aging Cell 18:e12933.

11. Lopes-Paciencia S, Saint-Germain E, Rowell M-C, et al. 2019. The senescence-associated secretory phenotype and its regulation. Cytokine 117:15–22.

12. Gresham RC, Kumar D, Copp J, et al. 2022. Characterization of induction and targeting of senescent mesenchymal stromal cells. Tissue Eng Part C Methods 28:239–249.

13. Kural KC, Tandon N, Skoblov M, et al. 2016. Pathways of aging: comparative analysis of gene signatures in replicative senescence and stress induced premature senescence. BMC Genom17:1030

14. Dierick JF, Eliaers F, Remacle J, et al. 2002. Stress-induced premature senescence and replicative senescence are different phenotypes, proteomic evidence. Biochem Pharmacol 64:1011–1017.

15. Tilton M, Liao J, Kim C, et al. 2025. Tracing cellular senescence in bone: time-dependent changes in osteocyte cytoskeleton mechanics and morphology. Small 21:2408517.

16. Gresham RC, Filler AC, Fok SW, et al. 2024. Compliant substrates mitigate the senescence associated phenotype of stress induced mesenchymal stromal cells. J Biomed Mater Res A 112:770–780.

17. Basisty N, Kale A, Jeon OH, et al. 2020. A proteomic atlas of senescence-associated secretomes for aging biomarker development. PLoS Biol 18:e3000599.

18. Ramos-Rodriguez DH, Leach JK. 2025. Decellularized cell-secreted extracellular matrices as biomaterials for tissue engineering. Small Sci 5:2400335.

19. Decaris ML, Leach JK. 2011. Design of experiments approach to engineer cell-secreted matrices for directing osteogenic differentiation. Ann Biomed Eng 39:1174–1185.

20. Harvestine JN, Orbay H, Chen JY, et al. 2018. Cell-secreted extracellular matrix, independent of cell source, promotes the osteogenic differentiation of human stromal vascular fraction. J Mater Chem B 6:4104–4115.

21. Kiernan J, Hu S, Grynpas MD, et al. 2016. Systemic mesenchymal stromal cell transplantation prevents functional bone loss in a mouse model of age-related osteoporosis. Stem Cells Transl Med 5:683–693.

22. Decaris ML, Binder BY, Soicher MA, et al. 2012. Cell-derived matrix coatings for polymeric scaffolds. Tissue Eng Part A 18:2148–2157.

23. Decaris ML, Mojadedi A, Bhat A, et al. 2012. Transferable cell-secreted extracellular matrices enhance osteogenic differentiation. Acta Biomater 8:744–752.

24. Xiong J, Dong L, Lv Q, et al. 2024. Targeting senescence-associated secretory phenotypes to remodel the tumour microenvironment and modulate tumour outcomes. Clin Transl Med 14:e1772.

25. Grotheer V, Skrynecki N, Oezel L, et al. 2021. Osteogenic differentiation of human mesenchymal stromal cells and fibroblasts differs depending on tissue origin and replicative senescence. Sci Rep 11:11968.

26. Fok SW, Gresham RCH, Ryan W, et al. 2023. Macromolecular crowding and decellularization method increase the growth factor binding potential of cell-secreted extracellular matrices. Front Bioeng Biotechnol 11:1091157–1091157.

27. Huang T, Yang M, Grant C, et al. 2025. Decellularized extracellular matrix produced by iPSC-derived MSCs promotes iPSC-MSC proliferation and differentiation and regulates secreted factors. J Biomed Mater Res A 113:e70010.

28. Cmielova J, Havelek R, Soukup T, et al. 2012. Gamma radiation induces senescence in human adult mesenchymal stem cells from bone marrow and periodontal ligaments. Int J Radiat Biol 88:393–404.

29. Hernandez-Segura A, Nehme J, Demaria M. 2018. Hallmarks of cellular senescence. Trends Cell Biol 28:436–453.

30. Liao E, Hsu Y, Chuah Q, et al. 2014. Radiation induces senescence and a bystander effect through metabolic alterations. Cell Death Dis 5:e1255–e1255.

31. Bertolo A, Baur M, Guerrero J, et al. 2019. Autofluorescence is a reliable in vitro marker of cellular senescence in human mesenchymal stromal cells. Sci Rep 9:2074.

32. Cramer MC, Badylak SF. 2020. Extracellular matrix-based biomaterials and their influence upon cell behavior. Ann Biomed Eng 48:2132–2153.

33. Molina MS, Brauer E, Günther R, et al. 2025. Increased substrate stiffness disrupts nuclear-cytoskeletal mechanical coupling in senescent cells. Mater Today Bio 35:102472.

34. Brauer E, Lange T, Keller D, et al. 2023. Dissecting the influence of cellular senescence on cell mechanics and extracellular matrix formation in vitro. Aging Cell 22:e13744.

35. Rapisarda V, Borghesan M, Miguela V, et al. 2017. Integrin beta 3 regulates cellular senescence by activating the TGF-β pathway. Cell Rep 18:2480–2493.

36. Sun AR, Ramli MFH, Shen X, et al. 2025. Hybrid hydrogel–extracellular matrix scaffolds identify biochemical and mechanical signatures of cardiac ageing. Nat Mater:1–13.

37. Lee Y, Shen X, Dreesen O, et al. 2025. Dysregulation of extracellular fibronectin and α5-integrin in dermal aging. Mol Biol Cell 36:ar99.

38. Hernandez-Segura A, de Jong TV, Melov S, et al. 2017. Unmasking transcriptional heterogeneity in senescent cells. Curr Biol 27(17):2652–2660.e4.

39. O'Hagan-Wong K, Nadeau S, Carrier-Leclerc A, et al. 2016. Increased IL-6 secretion by aged human mesenchymal stromal cells disrupts hematopoietic stem and progenitor cells' homeostasis. Oncotarget 7:13285.

40. Sun Y. 2023. An updated landscape of cellular senescence heterogeneity: Mechanisms, technologies and senotherapies. Transl Med Aging 7:46–51.

41. Zhang Y, Guo L, Han S, et al. 2020. Adult mesenchymal stem cell ageing interplays with depressed mitochondrial Ndufs6. Cell Death Dis 11:1075.

42. Jones S, Tai M, Ayushman M, et al. 2026. Donor variability and 3D culture models influence human mesenchymal stem cell differentiation. Tissue Eng Part A 32:43–53.

43. Choudhery MS, Badowski M, Muise A, et al. 2014. Donor age negatively impacts adipose tissue-derived mesenchymal stem cell expansion and differentiation. J Transl Med 12:8.

44. Muthamil S, Kim HY, Jang HJ, et al. 2024. Biomarkers of cellular senescence and aging: current state-of-the-art, challenges and future perspectives. Adv Biol 8:2400079.

45. Kapetanos K, Asimakopoulos D, Christodoulou N, et al. 2021. Chronological age affects MSC senescence in vitro-A systematic review. Int J Mol Sci 22(15):7945.

46. Kollmetz T, Castillo-Alcala F, Veale RWF, et al. 2025. Comparative analysis of commercially available extracellular matrix soft tissue bioscaffolds. Tissue Eng Part A 31:442–455.